CrossMark

# Room-temperature nanoimprint lithography to fabricate TiO$_2$ subwavelength phase retarder

**Zhehai Zhou[1] · Zhendong Zhu[2] · Lianqing Zhu[1]**

**Abstract**   A room-temperature nanoimprint lithography (RT-NIL) is presented to fabricate subwavelength phase retarders by combining high-refractive-index TiO$_2$ material, which shows some unique advantages in terms of lower cost, higher efficiency and better performances. The TiO$_2$ subwavelength phase retarders are designed and analyzed by the rigorous coupled wave analysis, where the phase retardations of 130° to 60° from 370 to 780 nm are achieved. The phase retarders are fabricated by the RT-NIL, where the fabrication process is described in details, and SEM images of fabricated gratings are shown. Further, phase retardations and transmittances of the fabricated phase retarders are measured, which shows that the transmittances of TE polarization and TM polarization are stronger than 76 % and 85 % in visible region respectively, and the measured phase retardations agree well with the theoretical results, and the proposed RT-NIL technique is expected to find wide applications in fabrication of subwavelength optical devices in future.

**Keywords**   Subwavelength phase retarder · Nanoimprint lithography · Phase retardation

✉ Zhehai Zhou
  zhouzhehai@bistu.edu.cn

✉ Zhendong Zhu
  zdzhu@mail.tsinghua.edu.cn

✉ Lianqing Zhu
  zhulianqing@sina.com

[1]   Beijing Key Laboratory for Optoelectronic Measurement Technology, Beijing Information Science and Technology University, Beijing 100192, China

[2]   State Key Laboratory of Precision Measurement Technology and Instruments, Tsinghua University, Beijing 100084, China

# 1 Introduction

Nanoimprint lithography (NIL) is well known for the capability of replicating nanostructures in large area with relatively lower cost and has been extensively explored to fabricate nano-to-microscale structures (Chou et al. 1996; Choi et al. 2013; Mori et al. 2009; Zhu et al. 2014; Päivänranta et al. 2008; Yu et al. 2011; Yamada et al. 2013; Wilson 2008), including subwavelength phase retarders on glass substrate (Mori et al. 2009). Because NIL produces nanopatterns by mechanical deformation in photoresist, the resolution can beyond the optical limitations associated with light diffraction. NIL has been regarded as a high-throughput and low-cost approach for patterning nanostructures over a wafer-scale area, and is widely considered as a future technique for the next generation semiconductors in the fields of electronics, optics, nanofluidics and biology.

In past decades, subwavelength phase retarders have been widely studied due to their interesting physical properties and wide applications. However, large retardation is difficult to achieve although many efforts have been made, such as the use of high-refractive-index dielectric materials (Isano et al. 2004; Isano et al. 2005; Saleem et al. 2013) and plasmonic subwavelength nanostructures (Chimento et al. 2011; Khoo et al. 2011; Gorodetski et al. 2012). Phase retarders with plasmonic subwavelength nanostructures have shown some advantages, involving miniature and integration, however, the inherent optical properties of metal ohmic loss and lower transmission limit their practical applications. As an alternative way, high-refractive-index dielectric materials, such as titanium oxide ($TiO_2$) adds impetus to alleviate the difficult. But it still requires a high-aspect-ratio grating structure with a small linewidth and a large grating step, so some nanofabrication factors are needed to consider, such as the etching conditions with some unexpected troubles (Isano et al. 2005). Therefore, the practical applications of subwavelength phase retarders are restricted due to the optical limitations, high cost and low throughput of traditional fabrication techniques, involving the photolithography and laser writing. In previous work, such functionalized nanostructures were usually fabricated by electron beam lithography (EBL) and focus-ion beam (FIB) etching. However, the relatively low yield and high cost cannot meet the practical requirements.
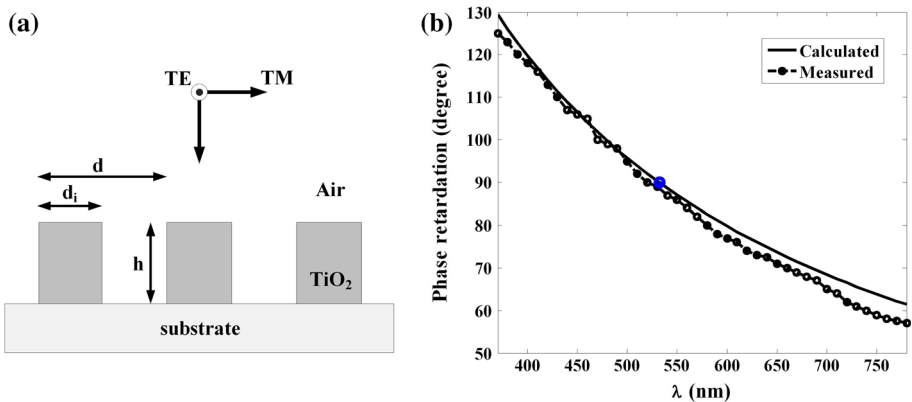


Fig. 1 **a** Schematic illustration of the phase retarder based on a subwavelength grating, **b** the calculated (*solid curve*) and measured (*dotted curve*) phase retardations in the visible range, where the *blue star* indicates the calculated phase retardation of 90° at 532 nm. (Color figure online)

In the paper, a room-temperature nanoimprint lithography (RT-NIL) is studied to fabricate subwavelength phase retarders by combining high-refractive-index TiO$_2$ material, by taking account of the low-cost, high efficiency and large area. The structural parameters and optical properties of the TiO$_2$ subwavelength phase retarders are theoretically simulated by the rigorous coupled wave analysis (RCWA). The fabrication of the devices based on RT-NIL is then described in details, and finally to evaluate the optical performances, the phase retardations and transmittances of the fabricated devices are measured from 370 to 780 nm to verify the feasibility of the fabrication technology.

## 2 Design and fabrication

The structure of the subwavelength phase retarder is illustrated in Fig. 1a, where parameters of the grating are defined as: $d$, the period, $d_i$, the line width of the grating, $f = d_i/d$, the fill factor, $h$, the depth of the grating. The phase retardation properties of the subwavelength grating are analyzed by the RCWA (Moharam and Gaylord 1981), where TE polarization is defined as the electric field parallel to the grating and the TM polarization is
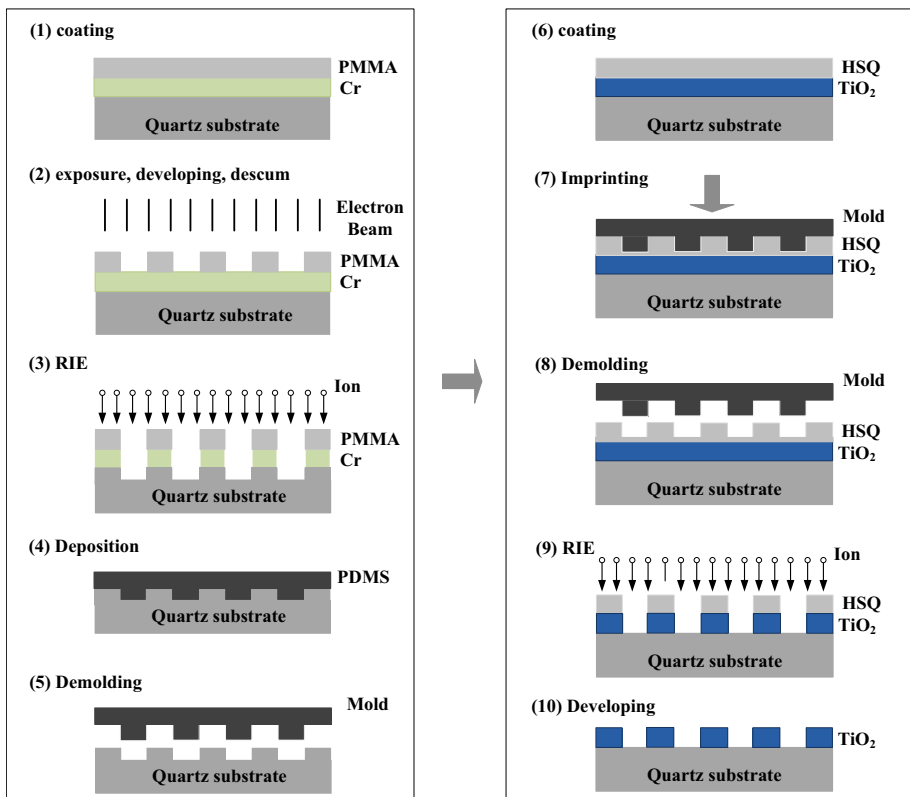


**Fig. 2** Basic process for fabrication of TiO$_2$ subwavelength phase retarders using nanoimprint technology, including two steps: the fabrication of mold (*left column*) and the room-temperature imprint lithography (*right column*)

that perpendicular to the grating. The fused silica quartz substrate is used, and the ambient medium is defined as air. The refractive index of the quartz substrate is 1.5, and the refractive index of the TiO$_2$ film is measured using an ellipsometer (Sentech, SE 400, Germany), which changes from 2.5 to 2.7 in the visible range. For the TiO$_2$ nanograting, it is expected that a strong grating diffraction produces the significant phase retardation. Figure 1b shows the simulated results of the phase retardation of the nanograting from 370 to 780 nm (the solid line), where the structure parameters are as follows: $d = 200$ nm, $d_i = 100$ nm, $f = 0.50$ and $h = 260$ nm. The phase retardations are approximately 130° and 62° at wavelengths of 370 and 780 nm respectively. Clearly, with the increasing of the wavelengths, the phase retardations decline. Especially, the phase retardation is 90° at 532 nm (as shown the circle marker), and the phase retardations are larger than 90° for wavelengths ranging from 350 to 532 nm.

To insight of the natural properties of the phase retardation, we manufacture the optical devices. Here, we developed a reliable RT-NIL technique to fabricate the TiO$_2$ subwavelength grating phase retarders. The fabrication process is sketched in Fig. 2, containing two parts: the left column illustrates the process of the mold fabrication, and the right one describes the room-temperature nanoimprint lithography (RT-NIL). The first part of the fabrication of the phase retarder is to manufacture the imprinting stamp: a thin layer of 40 nm Chromium (Cr) is deposited on the quartz substrate, following by the coating of a layer of electron beam (e-beam) photoresist PMMA under the prebaking condition of 105 °C and 3 min [Fig. 2(1)]. Then the resist is exposed by e-beam at the conditions of 1000 μC and 200 pA, and the pattern is transferred into the resist layer after developing. In order to remove the residual in the groove, a process of descum is carried out, with reactive ion etching (RIE) assisted by O$_2$ with a rate of flow 40 sccm, a pressure of 2 Pa, a RF power of 40 W and a processing time of 3 s [Fig. 2(2)]. Next, using the fabricated mask of PMMA, the layer of Cr is etched by RIE assisted by Cl$_2$ with a rate of flow 70 sccm, a pressure of 2 Pa, a RF power 70 W, and a processing time of 2 min. Sequentially, the etched Cr layer is used as a mask to further etch the layer of quartz substrate, using a RIE assisted by CF$_4$, with a rate of flow 40 sccm, a pressure of 2 Pa, a RF power of 70 W and a processing time of 8 min. The depth of etched groove is approximately 450 nm [Fig. 2(3)]. Then a mixture of an organosilicon polymer PDMS and a curing agent (SYLGARD 184, Down Corning Company, USA) is casted onto the etched quartz substrate, with a following process of a baking at 70 °C for 12 h [Fig. 2(4)]. Finally, the daughter mold is obtained after demolding of etched quartz substrate and patterned PDMS [Fig. 2(5)], working as the imprinting mold in the next process part.

The second part of the process is to manufacture the device of the subwavelength phase retarders. A layer of TiO$_2$ with 260 nm thick and a photoresist hydrogen silsequioxane (HSQ, XR-1541-006, Down Corning Company, USA) top layer with 150 nm are separately deposited on the quartz substrate [Fig. 2(6)]. Then, a RT-NIL process (50 psi, 7 min, at room temperature) is operated by using the PDMS daughter mold [Fig. 2(7)]. After demolding, the groove pattern is transferred onto the HSQ layer. A reaction ion etching (RIE) with pure CF$_4$ (40 sccm, 2 Pa, 40 W, 10 s) is to remove the HSQ residual in the imprinted grooves [Fig. 2(8)]. Then, with the nanopatterned HSQ mask, another RIE process is used to etch the TiO$_2$ layer in SF$_6$ plasma (48 sccm, 2 Pa, 40 W, 7 min) [Fig. 2(9)], and the pattern of the master stamp is transferred into the TiO$_2$ layer. Finally, the TiO$_2$ grating with a period of 200 nm and a depth of 260 nm is obtained by removal of HSQ resist using the mixed solution of sodium hydroxide (NaOH) and sodium chloride (NaCl) (the solution v/v = 1:10) [Fig. 2(10)]. The above process parameters are obtained

based on many trials and can be used to fabricate the designed grating structures with a good repeatability.

# 3 Results

The structure parameters of the fabricated samples are characterized by the scanning electron microscope (SEM, FEI Serion2000) images as shown in Fig. 3. The SEM image of the top morphology of the TiO$_2$ gratings is shown in Fig. 3a, which is the result of the first implemented RT-NIL with the original PDMS stamp. It also tells the truth that there are no any defects, such as collapsing, broken, and alignment errors, in the holistic field of the SEM view up to 1 mm$^2$, as well as the straight grating line Shown in Fig. 3b, the inset image shows a high resolution image of Fig. 3a, and indicates that the nanograting is the same with the original stamp ones, which also meets the requirement of the designed parameters of the period $d$ and the linewidth $d_i$. To analysis the depth of nanogratings, we also measure the cross-section image of the sample with the about 260 nm, as shown in Fig. 3c. The top layer of the Cr mask still holds on the raster line, which can be advantageous to achieve a rectangular TiO$_2$ grating. The profile of cross-section will determined the stable diffractive optical properties.
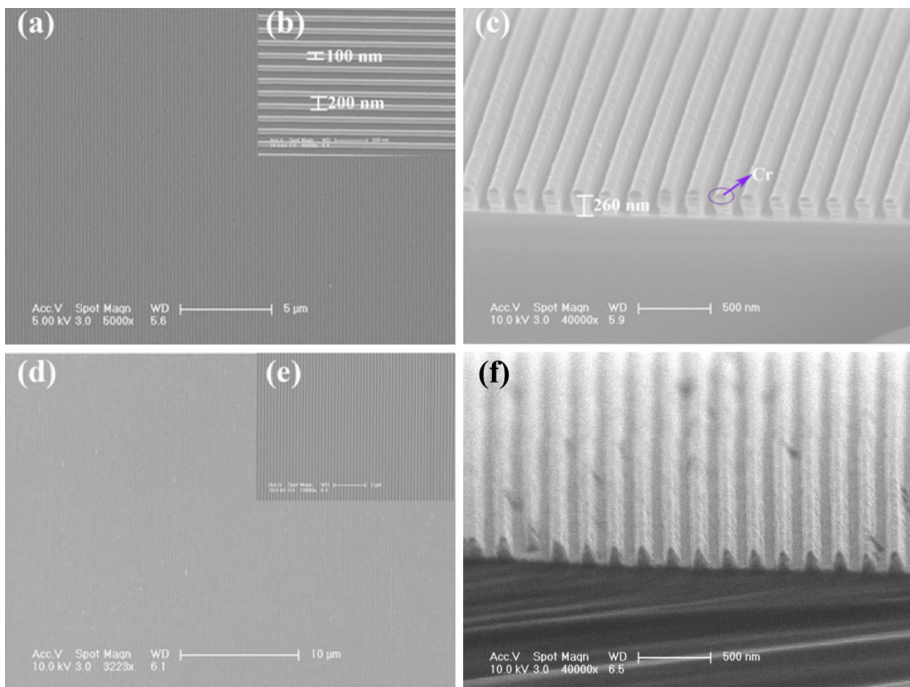


**Fig. 3** SEM images of the TiO$_2$ nanogratings, **a** the *top views* of grating grooves for the sample of the first RT-NIL implementation, the *inset* SEM image (**b**) with high resolution, the cross-section image (**c**) of (**a**), the *purple marks* in (**c**) shows the mask of the Cr layer. **d**, **e** The *top views* of the grating grooves for the sample of the 200th RT-NIL implementation using the same PDMS mold, and the *inset image* (**e**) and (**f**) are the large resolution and the cross-section images of (**d**), respectively. (Color figure online)

Furthermore, we investigate the repeatability of our developed RT-NIL technique to meet the requirements of the practical application. We also analysis the SEM images of the samples after implementing 200 recycles of RT-NIL with the same PDMS mold, the results are shown in Fig. 3d–f. Figure 3d, e is similar with the SEM image of Fig. 3a. We can find that even undergoing 200 recycles RT-NIL experiments, the top morphology still keeps on the constant with the original PDMS stamp, there are also no collapsing, broken even in the field of SEM view up to $\sim 2$ mm$^2$, which tells a good repeatability for our developed RT-NIL method. Figure 3f shows its side view of the grating grooves. Its top morphology of the raster line presents a little difference between Fig. 3c, because the sample was executed with an etching condition of SF$_6$ plasma (70 sccm, 2 Pa, 50 W, 7 min). So it does not obtain rectangular nanograting but triangular nanograting to achieve the desirable phase retardations. It is confirmed that the explored processing can easily fabricate nanograting devices with similar feature structures.

To evaluate the optical performances of fabricated nanogratings, both the phase retardations and transmittances of the fabricated nanograting devices with the trapezoidal profile (seeing Fig. 3f) are measured using a spectral analyzer (AvaSpec-ULS2048, Avantes Company). Figure 1b shows the measured phase retardations when the wavelengths ranging from 370 to 780 nm (the dotted line), which are good agreement with the calculated results. In the whole wavelength range, the measured results are a little smaller than calculated results, and the root mean square (RMS) variation is about 2.4°, especially the phase retardation is about 88.3° at 532 nm. The difference between calculated results and measured ones maybe comes from the height deviation and trapezoidal shape of nanogratings. Although a rectangular profile is in favor of achieving large phase retardations, it gives rise to an undesired Fresnel reflection at the gratings–air boundary. The effect can be minimized if the gratings structure has an etch profile of trapezoidal or triangular shape (Richter et al. 1995).
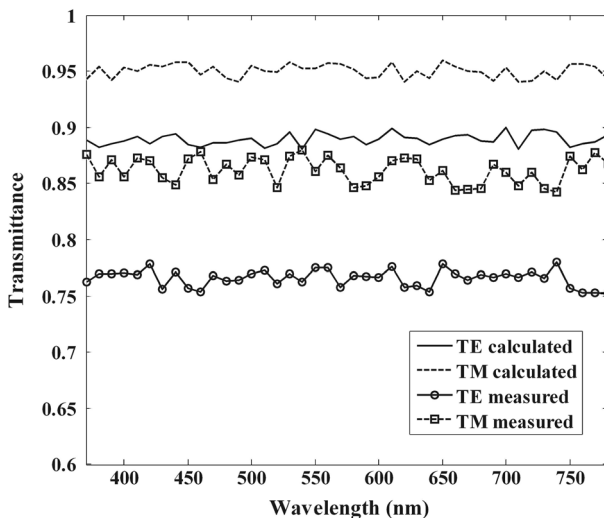


**Fig. 4** Calculated and measured transmittances of fabricated phase retarders for TE polarization and TM polarization in visible range (370–780 nm)

Figure 4 shows the results of the calculated transmittances and the measured ones of TE and TM polarized beams. The transmittances of TE polarization and TM polarization are stronger than 76 % and 85 % in visible region, respectively. Comparing with the calculated results, the measured average transmittances for TE polarization and TM polarization are lower about 12 % and 9 % respectively, which are mainly due to Fresnel reflections at the backside of the device.

## 4 Conclusion

In summary, we have demonstrated a RT-NIL technique to fabricate subwavelength TiO₂ phase retarders. By using RT-NIL technique and a high-refractive-index material of TiO₂, subwavelength phase retarders with high phase retardations in visible range have been achieved with high throughput and low cost. The phase retardations and transmittances of the fabricated devices are theoretically and experimentally demonstrated, which indicate that the experimental results agree well with the theoretical results, and the phase retardation changes of 130° to 60° from 370 to 780 nm are obtained, especially a phase retardation of 90° at wavelength of 532 nm. The technique based on RT-NIL can be extensively used to fabricate other subwavlength gratings devices, and may add impetus to the practical applications of subwavelength optical devices in optical instruments.

## References

Chimento, P., Kuzmin, N., Bosman, J., Alkemade, P., Hooft, G., Eliel, E.: A subwavelength slit as a quarter-wave retarder. Opt. Express **19**, 24219–24227 (2011)

Choi, J.H., Jo, H.B., Choi, H.J., Lee, H.: Fabrication of TiO₂ nano-to-microscale structures using UV nanoimprint lithography. Nanotechnology **24**, 195301 (2013)

Chou, S., Krauss, P., Renstrom, P.: Imprint lithography with 25-nanometer resolution. Science **272**, 85–87 (1996)

Gorodetski, Y., Lombard, E., Drezet, A., Genet, C., Ebbesen, T.W.: A perfect plasmonic quarter-wave plate. Appl. Phys. Lett. **101**, 201103 (2012)

Isano, T., Kaneda, Y., Iwakami, N., Ishizuka, K., Suzuki, N.: Fabrication of half-wave plates with sub-wavelength structures. Jpn. J. Appl. Phys. **43**, 5294–5296 (2004)

Isano, T., Kaneda, Y., Kadoshima, T., Ukaji, E., Sato, M., Ishizuka, K., Suzuki, N.: Improvement of phase retardation of wave plate with subwavelength structures by heat treatment. Jpn. J. Appl. Phys. **44**, 4984–4988 (2005)

Khoo, E., Li, E., Crozier, K.: Plasmonic wave plate based on subwavelength nanoslits. Opt. Lett. **36**(13), 2498–2500 (2011)

Moharam, M.G., Gaylord, T.K.: Rigorous coupled-wave analysis of planar-grating diffraction. J. Opt. Soc. A **71**(7), 811–818 (1981)

Mori, T., Yamashita, N., Kasa, H., Fukumi, K., Kintaka, K., Nishii, J.: Periodic sub-wavelength structures with large phase retardation fabricated by glass nanoimprint. J. Ceram. Soc. Jpn. **117**(10), 1134–1137 (2009)

Päivänranta, B., Passilly, N., Pietarinen, J., Laakkonen, P., Kuittinen, M., Tervo, J.: Low-cost fabrication of form-birefringent quarter-wave plates. Opt. Express **16**(21), 16334–16342 (2008)

Richter, I., Sun, P.C., Xu, F., Fainman, Y.: Design considerations of form birefringent microstructures. Appl. Opt. **34**(14), 2421–2429 (1995)

Saleem, M., Honkanen, S., Turunen, J.: Effect of substrate overetching and heat treatment of titanium oxide waveguide gratings and thin films on their optical properties. Appl. Opt. **52**, 422–432 (2013)

Wilson, B.K.: Variable wave plate via tunable form-birefringent structures. J. Microelectromech. Syst. **17**(4), 1039–1046 (2008)

Yamada, I., Yamashita, N., Einishi, T., Saito, M., Fukumi, K., Nishii, J.: Design and fabrication of an achromatic infrared wave plate with Sb–Ge–Sn–S system chalcogenide glass. Appl. Opt. **52**(7), 1377–1382 (2013)

Yu, C.C., Chen, Y.T., Wan, D.H., Chen, H.L., Ku, S.L., Chou, Y.F.: Using one-step, dual-side nanoimprint lithography to fabricate low-cost, highly flexible wave plates exhibiting broadband antireflection. Electrochem. Soc. **158**(6), J195–J199 (2011)

Zhu, Z.D., Bai, B., Duan, H.G., Zhang, H.S., Zhang, M.Q., You, O.B., Li, Q.Q., Tan, Q.F., Wang, J., Fan, S.S., Jin, G.F.: M-shaped grating by nanoimprinting: a replicable, large-area, highly active plasmonic surface-enhanced Raman scattering substrate with nanogaps. Small **10**(8), 1603–1611 (2014)